

Neoclassical and transport driven parallel SOL flows on TCV

R. A. Pitts, J. Horacek¹ and the TCV Team

École Polytechnique Fédérale de Lausanne (EPFL), Centre de Recherches en Physique des Plasmas, Association Euratom – Confédération Suisse, CH-1015 Lausanne, Switzerland

²Association EURATOM–Institute of Plasma Physics, Prague, Czech Republic

Introduction

Ion flows parallel to the magnetic field in the tokamak scrape-off layer (SOL) are now widely suspected to be an important player in the process of material migration, itself known to influence fuel retention [1]. In addition to the neoclassical (field direction dependent), Pfirsch-Schlüter (P-S) component [2], a second contribution receiving increasing attention is a field direction independent flow, thought to be a consequence of the ballooning nature of cross-field transport into the SOL. Previous experiments on TCV have measured the P-S component, demonstrating it to be of magnitude and direction expected by simple theory [3]. They have also clearly identified a possible “transport driven flow offset”, showing it to be of magnitude consistent with radial particle transport in the outboard SOL driven by convective interchange motions [3,4]. Nevertheless, given the chosen TCV magnetic equilibrium geometry and the measurement location *below* the outboard midplane of the discharge (see Fig. 1a), it was not possible in this earlier study to exclude a particle sink effect of the outer divertor target driving a parallel flow extending into the main SOL and of similar magnitude to that expected as a consequence of perpendicular transport. In new experiments, described here, the shape flexibility of TCV has been used to eliminate this contribution and to demonstrate the poloidally localized nature of the ballooning component. Further confirmation of the P-S flow component is also provided by these new measurements.

Experiment

The magnetic equilibria employed in the present study are shown in Fig.1b,c. All plasmas are ohmic L-mode with $I_p = 260$ kA, $R = 0.89$ m, $a \sim 0.24$ cm, $\delta_{95} \sim 0.3$, $\kappa_{95} \sim 1.5-1.6$. In each case, experiments are performed with both forward (FWD-B, ion $\mathbf{B} \times \nabla B$ drift downwards) and reversed (REV-B) toroidal field ($|B_\phi| = 1.43$ T). In all cases I_p is reversed with B_ϕ to preserve magnetic helicity. Apart from field direction and shape, the only variable parameter is plasma density, with discharge pairs in FWD and REV-B as closely matched as possible. Parallel flow profiles are measured with a 5-pin, fast reciprocating Mach probe (see

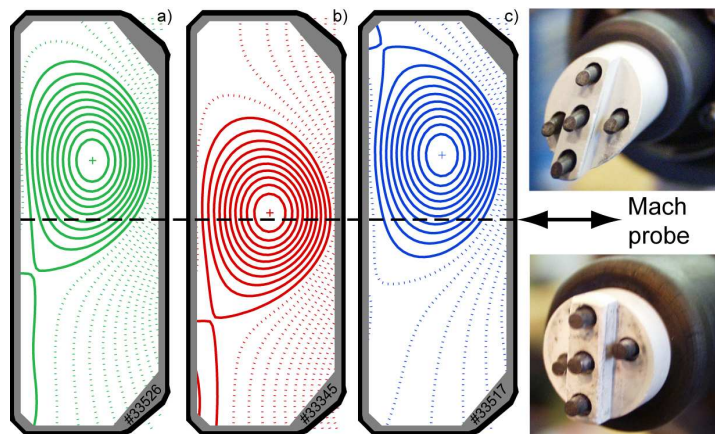


Fig. 1: Magnetic equilibria and reciprocating probe heads used for SOL flow studies. As indicated by the horizontal dashed line, the probe enters the plasma always on the machine midplane.

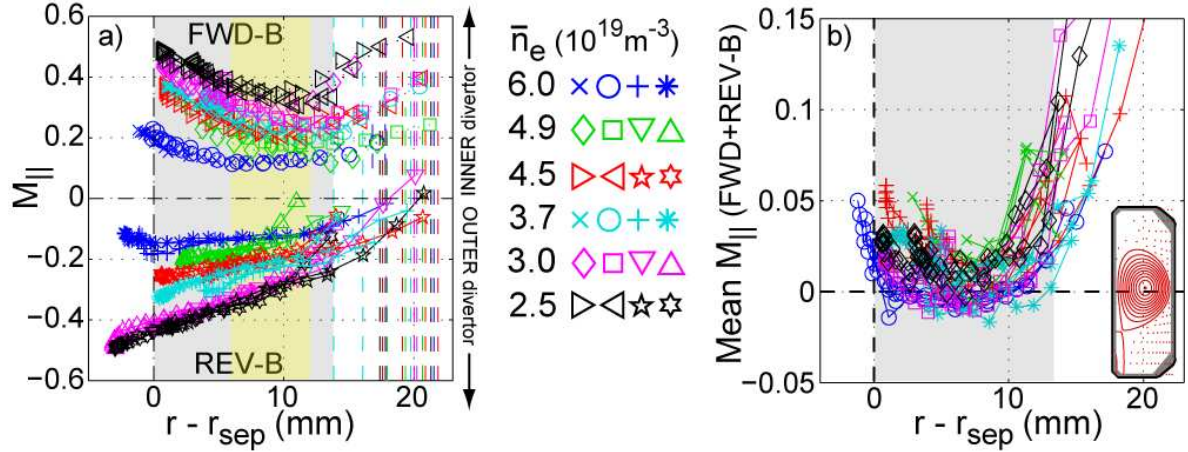


Fig. 2: a) Density scan of the parallel SOL flow radial profile in SNL for FWD and REV-B. The highest density is just below the density limit for this equilibrium and plasma current. b) Average profile of FWD-B and REV-B flows for each density.

photos in Fig. 1), entering the SOL plasma on the machine midplane. For the SNL discharge in Fig. 1b, this means that only a very thin radial slice of SOL plasma is sampled (~ 2 cm, see Fig. 2). In the case of the SNU configuration, flux expansion provides a wider SOL region. A dedicated probe head is required for each of the two equilibria to match the poloidal shape of magnetic surfaces. The central electrodes located on the bar separating the Mach pins are used both for turbulence measurements and to provide the radial profiles of local T_e , n_e and plasma potential, $\phi_p \sim V_f + 3T_e$, required for interpretation of the parallel flows. The Mach number, $M_{\parallel} = v_{\parallel}/c_s$, of the latter, is estimated in the usual way from the logarithmic ratio of ion saturation currents to the upstream and downstream pins. Ref. [3] provides more detail on the probe head and the methodology of these flow measurements.

Results

Fig. 2a compiles the flow profiles (mapped onto the outside midplane and given in distance from the separatrix) for the SNL configuration for both toroidal field directions and a 6-point density scan. The latter is performed discharge to discharge, with two probe reciprocations made in the stationary phase of each pulse, providing two separate profiles at any given density. The vertical dashed lines indicate the radial location of the first intersection point of a flux surface in the SOL with the outside wall at the midplane. Small differences in plasma position mean that this location changes slightly for each discharge. The grey shaded zones delimit the radial extent of the SOL region which connects fully from inner to outer target, whilst the yellow band corresponds to the narrow range of SOL width over which the experimental flows are compared with the theoretically expected P-S flow (see Fig. 4). In all figures, negative flows are directed *downwards*, positive flows *upwards*.

The flow profiles in Fig. 2a display all but one of the features already reported in [3] for measurements made in the SNL configuration of Fig.1a (namely ~ 23 cm below the midplane). The flow decreases with increasing density and increasing distance in the SOL, is directed towards the inner divertor for FWD-B, towards the outer target for REV-B and is thus always co-current. These directions are consistent with those seen in other tokamaks for

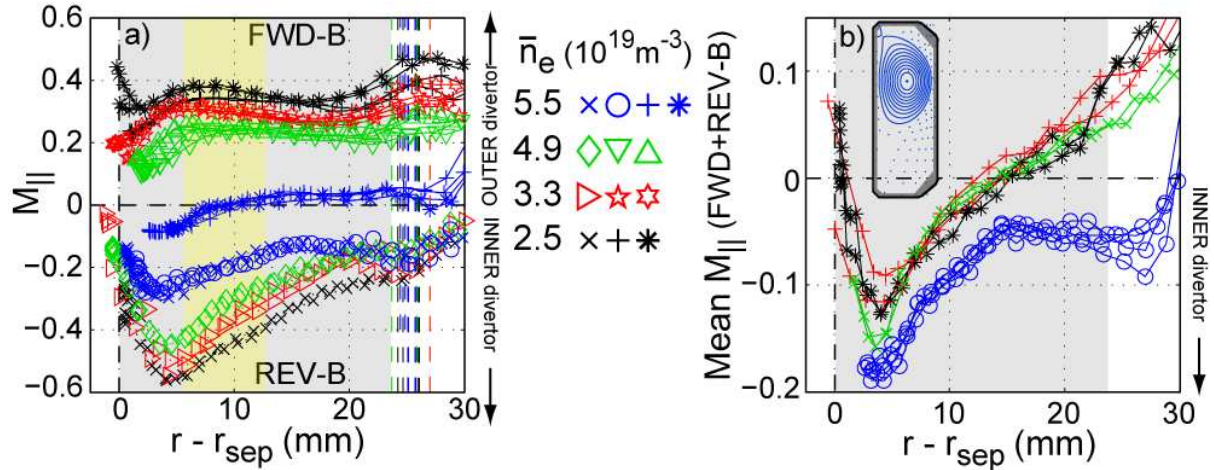


Fig. 3: a) Density scan of the parallel SOL flow radial profile in SNU for FWD and REV-B. b) Average profile of FWD-B and REV-B flows for each density.

measurements in similar poloidal locations and for given field direction. Crucially, the flows reflect almost symmetrically about zero for all densities, as shown in Fig.2b, which compiles the radial profiles of the average FWD and REV-B flows. For all densities and throughout the SOL, M_{\parallel} (mean) < 0.05 . Within the error bars of the measurement (not shown), this is essentially equivalent to a zero field independent flow component, as would be expected if the outboard midplane corresponded to a maximum in the perpendicular particle transport.

In [3], measurements below the midplane in the equilibrium of Fig.1a, revealed a field independent flow offset of magnitude $M_{\parallel} = 0.05 - 0.1$ directed towards the outer divertor, as expected if outboard transport in the midplane vicinity produced a local “over-pressure” above the probe location leading to parallel flow generation directed away from the midplane to both inner and outer divertors. The magnitude of this flow has been shown to be perfectly consistent with cross-field transport driven by interchange motions [3,4]. However, the open divertor geometry in TCV means that flow generation towards the target due to the target sink itself in configurations such as that in Fig.1a cannot be excluded as a cause of the field independent offset. Such flow of the right magnitude to account for the experiment is observed in SOLPS5 simulations without drifts [3]. The new SNL measurements in Fig. 2 tend to indicate that such target sink flows are in fact absent (but drift simulations, now underway, are required as confirmation). Proof that this is indeed the case is offered by the results in Fig. 3a, which illustrates the results of a density and field direction scan for the SNU equilibrium of Fig. 1c. In this case, the probe reciprocates into the SOL *above* the outer midplane of the discharge (relative to the X-point) and would therefore not expect to feel the presence of the outer divertor target sink. The field independent component, shown in Fig. 3b, nevertheless clearly shows a tendency throughout most of the SOL for a net flow downwards, now in the direction from outer to inner divertor. This is again consistent with a parallel flow pressure drive due to ballooning type radial transport and will not be influenced by the inner divertor sink since the target is much too far away. Again, SOLPS5 simulations of these plasmas, including drifts, are required to locate the flow stagnation points in the various

geometries. The field dependent flow components in Fig. 3a behave in similar fashion to those of Fig. 2a with regard to density and field direction dependence, but exhibit differences in radial profile. The “hump” seen in the profiles at $r - r_{\text{sep}} \sim 5$ mm is reminiscent of those reported from C-Mod for a similar probe location [5], but not thus far seen in TCV for SNL configurations.

Neoclassical flows: experiment versus theory

Turning to the field dependent flow, which Figs. 2 and 3 demonstrate to be the dominant component for all but the highest densities, a straightforward comparison can be made between experiment and the theoretically expected ion neoclassical P-S flow. An expression for the latter derived in the Appendix of [2] reduces to:

$$M_{\parallel}^{PS} = \frac{2q \cos \theta}{c_s} \left(E_r - \frac{\nabla p_i}{en_e} \right) \frac{\mathbf{B}}{B^2}$$

for large aspect ratio, cylindrical geometry. Here q is the cylindrical safety factor, θ the poloidal angle of the probe location ($\theta = 0$ defined for a probe at the midplane), E_r the radial electric field and p_i the ion pressure. Assuming $T_i = T_e$ and extracting E_r from $\nabla \phi_p$, the predicted and measured flows are shown in Fig. 4 for all SNL and SNU data in Figs. 2a and 3a. To improve the quality of gradients fitted through noisy experimental data and to account for the fact that full radial profiles are not available for each density, a 6 mm slice of the SOL over the range $6 \leq (r - r_{\text{sep}}) \leq 12$ mm (marked by the yellow bands in Figs. 2a, 3a) has been used to estimate the theoretical neoclassical flow. The field independent offset has been subtracted from the SNL data. Though there are some notable deviations, in general experiment and theory agree remarkably well, particularly when taking account of the simplifying assumptions invoked in the derivation of the theoretical expression. In common with the SNL equilibria in Fig. 1a for which the flows are reported in [3], it would thus appear that in steady-state, in the midplane vicinity, Pfirsch-Schlüter parallel flows compensating classical $E \times B$ and diamagnetic drifts can account fully for the measured toroidal field dependent flow on TCV.

Though there are some notable deviations, in general experiment and theory agree remarkably well, particularly when taking account of the simplifying assumptions invoked in the derivation of the theoretical expression. In common with the SNL equilibria in Fig. 1a for which the flows are reported in [3], it would thus appear that in steady-state, in the midplane vicinity, Pfirsch-Schlüter parallel flows compensating classical $E \times B$ and diamagnetic drifts can account fully for the measured toroidal field dependent flow on TCV.

Acknowledgement

This work was funded in part by the Swiss National Science Foundation. JH acknowledges support from the European Atomic Energy Community under an intra-European fellowship.

References

- [1] R. A. Pitts et al., Plasma Phys. Control. Fusion **47** (2005) B303
- [2] A. V. Chankin et al., accepted for publication in Nucl. Fusion (2007)
- [3] R. A. Pitts et al., J. Nucl. Mater. **363-365** (2007) 738
- [4] W. Fundamenski et al., Nucl. Fusion **47** (2007) 417
- [5] B. LaBombard et al., Nucl. Fusion **44** (2004) 1047

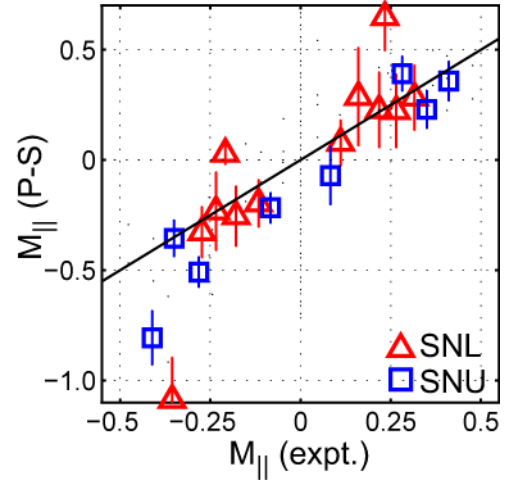


Fig. 4: Comparison of experimental and estimated neoclassical flows for the SNU and SNL plasmas.